

# A High-Resolution Detector in Multipath Environments

***Todd McWhorter***

Mission Research Corporation

phone: 970-282-4400

email: mcwhorter@aster.com

**Abstract** In this paper we introduce a high-resolution CFAR detector for the linear data model. The detector is derived using the generalized likelihood-ratio test (GLRT) framework. The resulting detector has a number of distinctive properties. One property of the detector is that it is most useful when the training and testing data contain the signal-of-interest. In fact, this detector does not need training data although it can utilize it if provided. This is in contrast to most methods, which in order to prevent signal suppression, require a set of signal-free training data to estimate the noise/interference background. Another important property of the detector is that the probability of detection is invariant to the correlation of the signal-of-interest with other signals. This can be particularly important in array processing, where the signal-of-interest is often correlated with one or more multipath components. If the objective of the detector is to discriminate between sources that are very close in terms of the spans of their signal subspaces, then the detector derived herein has very good resolution properties. In array processing, this translates to very good spatial resolution.

Report Documentation Page				Form Approved OMB No. 0704-0188	
Public reporting burden for the collection of information is estimated to average 1 hour per response, including the time for reviewing instructions, searching existing data sources, gathering and maintaining the data needed, and completing and reviewing the collection of information. Send comments regarding this burden estimate or any other aspect of this collection of information, including suggestions for reducing this burden, to Washington Headquarters Services, Directorate for Information Operations and Reports, 1215 Jefferson Davis Highway, Suite 1204, Arlington VA 22202-4302. Respondents should be aware that notwithstanding any other provision of law, no person shall be subject to a penalty for failing to comply with a collection of information if it does not display a currently valid OMB control number.					
1. REPORT DATE <b>20 DEC 2004</b>		2. REPORT TYPE <b>N/A</b>		3. DATES COVERED <b>-</b>	
4. TITLE AND SUBTITLE <b>A High-Resolution Detector in Multipath Environments</b>				5a. CONTRACT NUMBER	
				5b. GRANT NUMBER	
				5c. PROGRAM ELEMENT NUMBER	
6. AUTHOR(S)				5d. PROJECT NUMBER	
				5e. TASK NUMBER	
				5f. WORK UNIT NUMBER	
7. PERFORMING ORGANIZATION NAME(S) AND ADDRESS(ES) <b>Mission Research Corporation</b>				8. PERFORMING ORGANIZATION REPORT NUMBER	
9. SPONSORING/MONITORING AGENCY NAME(S) AND ADDRESS(ES)				10. SPONSOR/MONITOR'S ACRONYM(S)	
				11. SPONSOR/MONITOR'S REPORT NUMBER(S)	
12. DISTRIBUTION/AVAILABILITY STATEMENT <b>Approved for public release, distribution unlimited</b>					
13. SUPPLEMENTARY NOTES <b>See also, ADM001741 Proceedings of the Twelfth Annual Adaptive Sensor Array Processing Workshop, 16-18 March 2004 (ASAP-12, Volume 1)., The original document contains color images.</b>					
14. ABSTRACT					
15. SUBJECT TERMS					
16. SECURITY CLASSIFICATION OF:			17. LIMITATION OF ABSTRACT <b>UU</b>	18. NUMBER OF PAGES <b>10</b>	19a. NAME OF RESPONSIBLE PERSON
a. REPORT <b>unclassified</b>	b. ABSTRACT <b>unclassified</b>	c. THIS PAGE <b>unclassified</b>			

# A HIGH-RESOLUTION DETECTOR IN MULTI-PATH ENVIRONMENTS

*Todd McWhorter*

Mission Research Corporation  
3665 JFK Parkway  
Building 1, Suite 206  
Fort Collins, CO 80525  
Phone : 970-282-4400 x25  
Fax : 970-282-9444  
Email : mcwhorter@aster.com

## ABSTRACT

In this paper we introduce a high-resolution detector for the linear data-model. The detector is derived using the generalized-likelihood-ratio-test (GLRT) framework. The resulting detector has a number of distinctive properties. In particular, the detector is most-useful when the training and testing data *contain* the signal-of-interest. In fact, this detector does not need training data although it can utilize it if provided. This is in contrast to most methods, which in order to prevent signal suppression, require a set of signal-free training data to estimate the noise/interference background. Another important property of the detector is that the probability of detection is "nearly" invariant to the correlation of the signal-of-interest with other signals. This can be particularly important in array-processing where the signal-of-interest is often correlated with one or more multi-path components. If the objective of the detector is to discriminate between sources that are very close in terms of the spans of their signal subspaces, then the detector derived herein has very good resolution properties. In array processing this translates to very good spatial resolution.

## 1. INTRODUCTION

The generalized-likelihood-ratio test (GLRT) has been a useful tool for devising detectors in situations for which the distribution of the data contains unknown parameters. In this paper we derive a GLRT detector for the linear-model that extends and unifies previous work. We also enumerate the invariances of the detector and detail its properties. In particular when this detector is used to spatially-localize energy in array-processing scenarios, the results are nearly invariant to correlated multi-path.

---

This work supported by John Tague of ONR under contract N00014-00-C-0145.

Another useful characteristic of this detector is that it is applicable in cases where the training data contain the signal-of-interest. There are many situations for which this is a desirable property, especially if the interference is non-stationary over the span of the observations so that the training data do not exactly model the interference environment of the test data. This property is also useful when one can not guarantee signal-free training data. In the remainder of this paper we describe the underlying hypothesis test and derive the detector. This section is followed by a discussion of the properties of the detector. We conclude with some illustrative examples. The details of the rank-selection algorithm and derivations of the distributions of the detector will be deferred to a subsequent, more detailed, paper on these detectors.

## 2. HYPOTHESES AND DETECTOR

Let  $\mathbf{y}_i \in \mathbb{C}^N$  denote one of  $M$  vector-valued observations. We model these data by assuming that the signal-of-interest is embedded in additive noise and additive interference. Array snapshots and communication signals are often modeled this way and there are many other practical detection problems for which this model is appropriate. The hypotheses we consider in this paper are

$$\begin{aligned} H_1 : \mathbf{y}_i &\sim CN(\mathbf{H}\theta_i + \mathbf{S}\phi_i, \sigma^2\mathbf{I}) && \text{signal present} \\ H_0 : \mathbf{y}_i &\sim CN(\mathbf{S}\phi_i, \sigma^2\mathbf{I}) && \text{signal absent.} \end{aligned} \quad (1)$$

The matrix  $\mathbf{H} \in \mathbb{C}^{N \times p}$  describes the signal subspace  $\langle \mathbf{H} \rangle$  and the matrix  $\mathbf{S} \in \mathbb{C}^{N \times q}$  describes the interference subspace  $\langle \mathbf{S} \rangle$ . We implicitly assume that these subspaces have been whitened by any *known* noise coloring. That is, if the noise covariance matrix was originally  $\sigma^2\mathbf{R}$ , with  $\text{tr}\{\mathbf{R}\} = N$ , then we modify the model components as such:  $\mathbf{y}_i \leftarrow \mathbf{R}^{-1/2}\mathbf{y}_i$ ,  $\mathbf{H} \leftarrow \mathbf{R}^{-1/2}\mathbf{H}$ ,  $\mathbf{S} \leftarrow$

$\mathbf{R}^{-1/2}\mathbf{S}$ . Frequently, a distribution for  $\boldsymbol{\phi}_i$  is assumed. In this instance the interference component is usually modeled as a term that colors the covariance matrix. We emphasize that this is not the assumption we make here. The "noise coloring" we describe above is not from interfering sources. Instead we model the amplitude vectors  $\boldsymbol{\theta}_i \in \mathbb{C}^p$  and  $\boldsymbol{\phi}_i \in \mathbb{C}^q$  as unknown but deterministic. We argue that in cases where  $M$  is "small", there are not enough data vectors to statistically-model the mode amplitudes with any degree of confidence. For example the interference amplitude vector  $\boldsymbol{\phi}_i$  has dimension  $q$ . Using a widely-quoted rule-of-thumb, this implies that we need approximately  $M = 3q$  snapshots to "satisfactorily" estimate the covariance matrix of  $\boldsymbol{\phi}$  — provided that this vector was truly Gaussian in the first place! By small  $M$  we mean  $M < 3q$ , although the results are certainly applicable for larger  $M$ .

We assume that the signal and interference amplitude vectors  $\boldsymbol{\theta}_i \in \mathbb{C}^p$  and  $\boldsymbol{\phi}_i \in \mathbb{C}^q$  are unknown for each data vector. We also assume that the noise power  $\sigma^2$  is unknown. Finally, we assume that the interference subspace  $\langle \mathbf{S} \rangle$  is also unknown. It is this final assumption that distinguishes this detector from those of Scharf and Friedlander [1]. To reiterate the only known quantity in this test is the subspace of the signal-of-interest  $\langle \mathbf{H} \rangle$ . Finally we assume that the data vectors are pair-wise independent. The derivation of the detector is similar to that presented [1]. Let  $\mathbf{Y} = [\mathbf{y}_1 \ \mathbf{y}_2 \ \cdots \ \mathbf{y}_M]$  denote the  $N \times M$  data matrix. Consider first the null hypothesis. The maximum-likelihood estimates of the interference amplitudes are

$$\hat{\boldsymbol{\phi}}_i = (\mathbf{S}^* \mathbf{S})^{-1} \mathbf{S}^* \mathbf{y}_i; \quad (\text{under } H_0).$$

The joint likelihood-function for the data can be compressed with these estimates to yield

$$\begin{aligned} f_0(\mathbf{Y}; \{\hat{\boldsymbol{\phi}}_i\}_1^M, \sigma^2, \mathbf{S}) &= \frac{1}{(\pi \sigma^2)^{MN}} \exp \left[ -\frac{1}{\sigma^2} \sum_{i=1}^M \mathbf{y}_i^* (\mathbf{I} - \mathbf{P}_\mathbf{S}) \mathbf{y}_i \right] \\ &= \frac{1}{(\pi \sigma^2)^{MN}} \exp \left[ -\frac{1}{\sigma^2} \text{tr} \{ (\mathbf{I} - \mathbf{P}_\mathbf{S}) \sum_{i=1}^M \mathbf{y}_i \mathbf{y}_i^* (\mathbf{I} - \mathbf{P}_\mathbf{S}) \} \right] \\ &= \frac{1}{(\pi \sigma^2)^{MN}} \exp \left[ -\frac{M}{\sigma^2} \text{tr} \{ (\mathbf{I} - \mathbf{P}_\mathbf{S}) \hat{\mathbf{R}} (\mathbf{I} - \mathbf{P}_\mathbf{S}) \} \right]. \quad (2) \end{aligned}$$

Here  $\mathbf{P}_\mathbf{S} = \mathbf{S}(\mathbf{S}^* \mathbf{S})^{-1} \mathbf{S}^*$  is an orthogonal projection matrix and

$$\hat{\mathbf{R}} = \frac{1}{M} \sum_{i=1}^M \mathbf{y}_i \mathbf{y}_i^*$$

is the sample covariance matrix. In (2) we have used the notation of [1] and listed the unknown and compressed

parameters in the argument of the likelihood-function. The maximum-likelihood estimate of the noise power is

$$\hat{\sigma}^2 = \frac{1}{N} \text{tr} \{ (\mathbf{I} - \mathbf{P}_\mathbf{S}) \hat{\mathbf{R}} (\mathbf{I} - \mathbf{P}_\mathbf{S}) \},$$

which results in a compressed likelihood-function

$$f_0(\mathbf{Y}; \{\hat{\boldsymbol{\phi}}_i\}_1^M, \hat{\sigma}^2, \mathbf{S}) = \left( \frac{MN}{e\pi} \right)^{MN} \times \cdots \left( \frac{1}{\text{tr} \{ (\mathbf{I} - \mathbf{P}_\mathbf{S}) \hat{\mathbf{R}} (\mathbf{I} - \mathbf{P}_\mathbf{S}) \}} \right)^{MN}.$$

Finally, it remains to estimate the interference subspace. It is not difficult to show that the maximum likelihood estimate of  $\mathbf{S}$  is the rank- $q$  dominant subspace of  $\hat{\mathbf{R}}$ . Herein we denote the ordered eigenvalues of a matrix  $\mathbf{A}$  by  $\lambda_1\{\mathbf{A}\} \geq \lambda_2\{\mathbf{A}\} \geq \cdots \geq \lambda_N\{\mathbf{A}\}$ . In our case we are interested in the eigenvalues of  $\hat{\mathbf{R}}$ . Define  $L = \min(M, N)$ . When  $M < N$  some of these eigenvalues will be zero and the spectrum can be more efficiently computed from the singular-value decomposition of the data matrix  $\mathbf{Y}$ . In any case, compressing the likelihood-ratio with the estimate for  $\mathbf{S}$  yields

$$f_0(\mathbf{Y}; \{\hat{\boldsymbol{\phi}}_i\}_1^M, \hat{\sigma}^2, \hat{\mathbf{S}}) = \left( \frac{MN}{e\pi} \right)^{MN} \times \cdots \left( \frac{1}{\sum_{i=q+1}^L \lambda_i \{\hat{\mathbf{R}}\}} \right)^{MN} \quad (3)$$

Now assume hypothesis  $H_1$  is in force. The procedures for estimating the mode amplitudes and the noise power in this case are identical to those used above. Consequently, we present the partially-compressed likelihood-function

$$f_1(\mathbf{Y}; \{\hat{\boldsymbol{\phi}}_i\}_1^M, \{\hat{\boldsymbol{\theta}}_i\}_1^M, \hat{\sigma}^2, \mathbf{S}) = \left( \frac{MN}{e\pi} \right)^{MN} \times \cdots \left( \frac{1}{\sum_{i=1}^M \mathbf{y}_i^* (\mathbf{I} - \mathbf{P}_{\mathbf{H}\mathbf{S}}) \mathbf{y}_i} \right)^{MN} \quad (4)$$

without derivation. Our next step is to factor the projection matrix  $\mathbf{P}_{\mathbf{H}\mathbf{S}}$  as

$$\mathbf{P}_{\mathbf{H}\mathbf{S}} = \mathbf{P}_\mathbf{H} + (\mathbf{I} - \mathbf{P}_\mathbf{H}) \mathbf{S} (\mathbf{S}^* (\mathbf{I} - \mathbf{P}_\mathbf{H}) \mathbf{S})^{-1} \mathbf{S}^* (\mathbf{I} - \mathbf{P}_\mathbf{H}).$$

Recall that  $\mathbf{H} \in \mathbb{C}^{N \times p}$  is known. This is essentially the factorization in [1] except that here we separate the projection using the signal subspace as the "reference" instead of the interference subspace. Now factor the projection matrix

$$\mathbf{I} - \mathbf{P}_\mathbf{H} = \mathbf{A} \mathbf{A}^*; \quad \mathbf{A} \in \mathbb{C}^{N \times N-p}, \quad \mathbf{A}^* \mathbf{A} = \mathbf{I}$$

and define

$$\mathbf{z}_i = \mathbf{A}^* \mathbf{y}_i; \quad \tilde{\mathbf{S}} = \mathbf{A}^* \mathbf{S} \in \mathbb{C}^{(N-p) \times q}.$$

We also define the new sample covariance matrix

$$\hat{\mathbf{R}}_{zz} = \frac{1}{M} \sum_{i=1}^M \mathbf{z}_i \mathbf{z}_i^*.$$

These definitions can be incorporated into (4) to yield

$$f_1(\mathbf{Y}; \{\hat{\boldsymbol{\phi}}_i\}_1^M, \{\hat{\boldsymbol{\theta}}_i\}_1^M, \hat{\sigma}^2, \tilde{\mathbf{S}}) = \left( \frac{MN}{e\pi} \right)^{MN} \times \dots \left( \frac{1}{\text{tr}\{\hat{\mathbf{R}}_{zz} - \mathbf{P}_{\tilde{\mathbf{S}}} \hat{\mathbf{R}}_{zz} \mathbf{P}_{\tilde{\mathbf{S}}}\}} \right)^{MN}. \quad (5)$$

The maximum-likelihood estimate of  $\tilde{\mathbf{S}}$  is the rank- $q$  dominant subspace of  $\hat{\mathbf{R}}_{zz}$ . Compressing the likelihood-function with this estimate gives

$$f_1(\mathbf{Y}; \{\hat{\boldsymbol{\phi}}_i\}_1^M, \{\hat{\boldsymbol{\theta}}_i\}_1^M, \hat{\sigma}^2, \hat{\tilde{\mathbf{S}}}) = \left( \frac{MN}{e\pi} \right)^{MN} \times \dots \left( \frac{1}{\sum_{i=q+1}^L \lambda_i \{\hat{\mathbf{R}}_{zz}\}} \right)^{MN}. \quad (6)$$

Since, in the algorithm that follows, we never explicitly compute  $\hat{\mathbf{R}}_{zz}$ , we will write (6) in the equivalent, and more intuitive, form

$$f_1(\mathbf{Y}; \{\hat{\boldsymbol{\phi}}_i\}_1^M, \{\hat{\boldsymbol{\theta}}_i\}_1^M, \hat{\sigma}^2, \hat{\tilde{\mathbf{S}}}) = \left( \frac{MN}{e\pi} \right)^{MN} \times \dots \left( \frac{1}{\sum_{i=q+1}^L \lambda_i \{(\mathbf{I} - \mathbf{P}_{\mathbf{H}}) \hat{\mathbf{R}} (\mathbf{I} - \mathbf{P}_{\mathbf{H}})\}} \right)^{MN}. \quad (7)$$

It is understood that only  $L - p = \min(M, N) - p$  eigenvalues will be non-zero. The generalized likelihood-ratio is formed by dividing the likelihood function under  $H_1$  in (7) by the likelihood-function under  $H_0$  in (3). It is easy to show that this detector is a monotonic function of

$$s = \frac{\sum_{q+1}^L \lambda_i \{\hat{\mathbf{R}}\}}{\sum_{q+1}^L \lambda_i \{(\mathbf{I} - \mathbf{P}_{\mathbf{H}}) \hat{\mathbf{R}} (\mathbf{I} - \mathbf{P}_{\mathbf{H}})\}}, \quad (8)$$

which implies that the detector in (8) is equivalent to the GLRT detector. In the simulations that follow this detector is designated by the acronym CAPE. The reason for this nomenclature is that the *equivalent* detector

$$c = MN \log(s) \quad (9)$$

can be interpreted as a capacity estimator.

It should be noted that while the CAPE statistic is based on energy in the sub-dominant ("noise") subspace,

this algorithm is *not* MUSIC [2]. Recall that MUSIC performs one spectral decomposition for all look-directions, whereas it is necessary to take a new spectral decomposition for each look direction in CAPE. We will argue in the next section that it is this step that allows CAPE to have high-resolution and resistance to both multi-path and mismatch. In Section 4 we describe how this extra computational burden can be reduced.

We also would like to emphasize that this detector is not equivalent to the SSMUSIC direction-of-arrival estimator described by McCloud and Scharf [3]. Again, the easiest way to distinguish these two statistics is that SSMUSIC requires only one spectral decomposition regardless of the number of look-directions.

### 3. DETECTOR PROPERTIES

In essence, the CAPE detector is based on observing the change in the data when the signal-of-interest is *removed* from the data. This is in contrast to *matched* detectors, which "measure" the change in the data when the signal-of-interest is present. This fundamental difference has some important practical consequences. The matched detectors require signal-free training data to determine the quiescent or background state. It is only when this background is characterized can these detectors measure the change that occurs if the signal-of-interest is present. In contrast the  $H_1$  hypothesis underlying the CAPE detector assumes that the signal-of-interest is present in all the data. Consequently, signal-free training data are not required for the CAPE detector.

The first important property of the detector in (9) is that it is invariant to a complex-scaling of the data matrix  $\mathbf{Y} = [\mathbf{y}_1 \dots \mathbf{y}_M]$ . Therefore the distribution of the statistic under the null hypothesis is independent of the noise power. Detectors that possess this property are commonly called constant-false-alarm-rate (CFAR) detectors. However to be truly CFAR, a detector must be invariant to *all* parameters that are unknown under the null hypothesis. In this case, a CFAR detector would be required to be invariant to the unknown interference subspace  $\langle \mathbf{S} \rangle$  and the amplitudes of the interference components  $\{\boldsymbol{\phi}_i\}$ . Unfortunately, the CAPE detector does not possess these invariances and the author believes that it is most-likely impossible to design any meaningful detector that does. However, as we show in the simulations, the CAPE detector is remarkably resistant to the effects of the interference. As a quick explanation, strong interference effects are generally manifested in the dominant subspace of the sample covariance matrix. However, the CAPE statistic examines energy only in the sub-dominant subspace. Of course with  $M$  finite, any interference component will affect all the eigenvalues of the sample co-

variance matrix, so we can never be truly invariant to its effects. Finally we note that if the detector is operated in "search mode" where the detector output is compared for a number of different signal subspaces  $\langle \mathbf{H} \rangle$ , the lack of a truly CFAR property is less important since the presence or absence of a signal is inferred not solely by the amplitude of the statistic but by its value relative to the other "search" directions.

Another important property of the detector is that it is robust to correlations between the signal-of-interest and signals in a different subspace. This property can be particularly important for detecting the presence of weak multi-path signals in array-processing problems. To see this, let's consider a simple array-processing example where the data vectors (snapshots) are composed of two correlated signals

$$\mathbf{y}(k) = \mathbf{a}_1 \theta_1(k) + \mathbf{a}_2 \theta_2(k) + \mathbf{n}(k). \quad (10)$$

Here  $\mathbf{a}_1$  and  $\mathbf{a}_2$  are the unit-norm array-response vectors for the signal-of-interest and a multi-path component. The assumption is that the amplitudes  $\theta_1(k)$  and  $\theta_2(k)$  are correlated. The effect of correlated multi-path is to introduce mismatch into the array-response vectors. This mismatch reduces the output-response of "matched" detectors since the assumed array-response differs from the actual array-response, which has changed because of interference-pattern effects. In contrast the CAPE detector "removes" the signal-of-interest so any correlations this signal may or may not have with any other signals has no effect on the denominator in (8) and minimal effect on the numerator.

#### 4. COMPUTATION

In this section we examine methods for reducing the computational-load in forming the CAPE statistic of (8). The implicit assumption of this section is that the statistic will be computed for a number of "look-directions/subspaces"  $\mathbf{H}$ . That is, the detector is "scanned" over a range of possible signals-of-interest. The first, somewhat obvious point, is that the numerator of the statistic in (8) is independent of  $\mathbf{H}$  and needs only to be computed once regardless of how many "look-directions" are used. Secondly, the overhead associated with the spectral-decomposition in the denominator of (8) can be reduced in two ways. Denote the singular-value-decomposition (SVD) of the data matrix as

$$\mathbf{Y} = [\mathbf{y}_1 \ \mathbf{y}_2 \ \cdots \ \mathbf{y}_M] = \mathbf{U}\mathbf{S}\mathbf{V}^*.$$

(Note this spectral decomposition is available from computing the numerator term.) The denominator term can be found from the singular-values of

$$(\mathbf{I} - \mathbf{P}_h)\mathbf{Y} = (\mathbf{I} - \mathbf{h}\mathbf{h}^*)\mathbf{U}\mathbf{S}\mathbf{V}^* \quad (11)$$

where we have assumed a rank-one signal subspace. The results herein can be easily generalized to accommodate higher-dimensional subspaces. At this point we also assume that the spectral-decomposition of  $\mathbf{Y}$  is not in compact form, i.e. the matrix  $\mathbf{U}$  is  $N \times N$  and unitary and  $\mathbf{S}$  may have some zeros on the diagonal. The expression in (11) can be written as

$$\begin{aligned} (\mathbf{I} - \mathbf{P}_h)\mathbf{Y} &= (\mathbf{I} - \mathbf{h}\mathbf{h}^*)\mathbf{U}\mathbf{S}\mathbf{V}^* \\ &= \mathbf{U}(\mathbf{S} - \mathbf{U}^*\mathbf{h}\mathbf{h}^*\mathbf{U}\mathbf{S})\mathbf{V}^* \\ &\triangleq \mathbf{U}(\mathbf{S} - \mathbf{w}\mathbf{w}^*\mathbf{S})\mathbf{V}^* \end{aligned} \quad (12)$$

where we have defined the unit-norm vector  $\mathbf{w} = \mathbf{U}^*\mathbf{h}$ . Using the technique of Schreiber [4], define the magnitude and phase factors  $\mathbf{w} = \mathbf{D}\mathbf{m}$  where  $w_i = m_i e^{j\phi_i}$ ,  $\mathbf{m} = [m_1 \ \cdots \ m_N]^T$  is a length  $N$  unit-norm real-valued vector, and  $\mathbf{D} = \text{diag}\{e^{j\phi_1}, \dots, e^{j\phi_N}\}$ . We can now write (12) as

$$\begin{aligned} (\mathbf{I} - \mathbf{P}_h)\mathbf{Y} &= \mathbf{U}(\mathbf{S} - \mathbf{w}\mathbf{w}^*\mathbf{S})\mathbf{V}^* \\ &= \mathbf{U}(\mathbf{S} - \mathbf{D}\mathbf{m}\mathbf{m}^T\mathbf{D}^*\mathbf{S})\mathbf{V}^* \\ &= \mathbf{U}\mathbf{D}(\mathbf{S} - \mathbf{m}\mathbf{m}^T\mathbf{S})\mathbf{D}^*\mathbf{V}^*. \end{aligned} \quad (13)$$

This equation indicates that singular-values of the complex-valued matrix  $(\mathbf{I} - \mathbf{P}_h)\mathbf{Y}$  are equal to the singular-values of the real-valued matrix  $\mathbf{S} - \mathbf{m}\mathbf{m}^T\mathbf{S}$ . There are many methods for efficiently computing the singular-values of a diagonal plus rank-one outer-product or, equivalently, the eigenvalues of the symmetric, diagonal plus rank-one outer-product

$$\begin{aligned} (\mathbf{S} - \mathbf{m}\mathbf{m}^T\mathbf{S})^T(\mathbf{S} - \mathbf{m}\mathbf{m}^T\mathbf{S}) &= \mathbf{S}^2 - \mathbf{S}\mathbf{m}\mathbf{m}^T\mathbf{S} \\ &\triangleq \mathbf{S}^2 - \boldsymbol{\mu}\boldsymbol{\mu}^T \end{aligned} \quad (14)$$

where we have defined  $\boldsymbol{\mu} \triangleq \mathbf{S}\mathbf{m}$ .

Finally, we can exploit the fact that often the look-directions are scanned in a manner such that adjacent look-directions are "close" (perhaps in the sense of a small principal angle although an exact definition of the norm is not necessary). Consequently, the associated spectral-decompositions are often close in some matrix norm. Since spectral-decomposition is an iterative process, the spectral-decomposition of the adjacent look-direction can be used as an initial value in the new decomposition — a procedure that can significantly reduce the number of required iterations. Moreover, we are only interested in the sum of the sub-dominant eigenvalues. We can determine this quantity by taking the trace of the matrix minus the sum of the dominant eigenvalues. Consequently, it is only necessary to compute the dominant eigenvalues. This is advantageous for two reasons. First, because the dominant eigenvalues tend to converge

more quickly than the sub-dominant ones and second, the size of the interference (dominant) subspace  $q$  is often small in comparison to  $\min(M, N)$ . An algorithm that performs adequately, and the one used to compute the numerical examples in this paper, is the orthogonal iteration algorithm [5].

#### Computing CAPE with the orthogonal iteration algorithm

1. Compute the SVD of  $\mathbf{Y}$

$$\mathbf{Y} = \mathbf{U}\mathbf{S}\mathbf{V}^* = [\mathbf{Q}_0 \ \mathbf{U}_{sd}] \begin{bmatrix} \mathbf{S}_d & \mathbf{0} \\ \mathbf{0} & \mathbf{S}_{sd} \end{bmatrix} \begin{bmatrix} \mathbf{V}_0^* \\ \mathbf{V}_{sd}^* \end{bmatrix}.$$

where  $\mathbf{Q}_0 \in \mathbb{C}^{N \times q}$  is the initial dominant subspace.

2. Compute the numerator of the statistic:  $n = \text{tr}(\mathbf{S}_{sd}^2)$ .
3. For each look direction  $\mathbf{h}_i$ ,  $i = 1, 2, \dots, B$ .
  - (a) Compute  $\mathbf{m} = \text{mag.}(\mathbf{U}^* \mathbf{h}_i)$ ,  $\boldsymbol{\mu} = \mathbf{S} \mathbf{m}$ .
  - (b) Initialize the dominant subspace using the previous iteration's estimate  $\mathbf{Q}_i = \mathbf{Q}_{i-1}$ .
  - (c) Perform an orthogonal iteration
    - i.  $\mathbf{A} = (\mathbf{S}^2 - \boldsymbol{\mu} \boldsymbol{\mu}^T) \mathbf{Q}_i$
    - ii.  $\mathbf{Q} \mathbf{T} = \mathbf{A}$  (QR factorization)
    - iii.  $\mathbf{Q}_i \leftarrow \mathbf{Q}$
  - (d) Repeat c) until the relative change in  $\text{tr}(\mathbf{T})$  is less than  $\epsilon$ .
  - (e) Compute the CAPE statistic

$$d_i = n / (\text{tr}(\mathbf{S}^2) - \text{tr}(\mathbf{T})) \quad \text{or} \\ c_i = \ln(n) - \ln(\text{tr}(\mathbf{S}^2) - \text{tr}(\mathbf{T})).$$

In the simulations of this paper, the algorithm typically required only 2 iterations to converge (with  $\epsilon = 10^{-4}$ ) unless the new look-direction was in close proximity to a source.

## 5. SIMULATIONS

In this section we assume that the data are obtained from an  $N = 50$  element, uniform linear array. The nominal element spacing is 1 meter with an assumed wavefront velocity of 1500 meters/second. The element positions are perturbed by adding independent Gaussian random variables to each of the elements' three coordinates. Detection statistics are formed for 201 equally-spaced, in cosine space, look-directions (beams). In the first simulation we have two closely-spaced (beams 20 and 30)

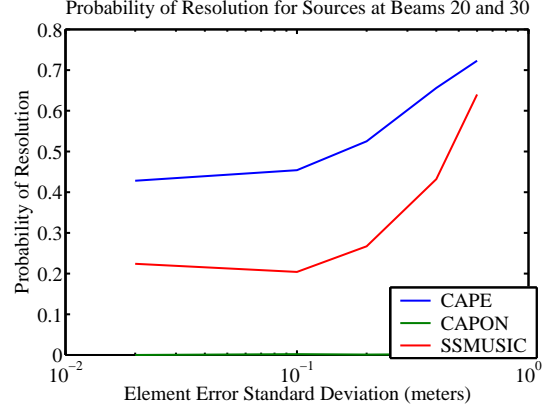


Figure 1: Probability of Resolution Results

sources with array-output SNRs of 13 and 3 dB respectively. A third, low-power source (output SNR of -4 dB), is nominally on beam 80. All sources are narrowband with a frequency of 20 percent of the array design frequency. In Figure 1 we plot the probability of resolution versus the standard deviation of the element perturbation "noise". We consider the two sources on beams 20 and 30 resolved if the detector outputs on these beams are larger than the minimum of the detector outputs on the intervening beams 21-29. The CAPE detector has substantially better resolution properties until the array mismatch is so great that the probability of detection approaches the value that would be obtained using white-noise instead of the detector outputs to make the resolution decision.  $M = 10$  snapshots were used per trial, with the statistics gathered over 1000 trials at each value of array mismatch.

In Figure 2, we plot an average peak-picked, detector response versus bearing for this same experiment. For each trial we compute the detector output for the given number of beams. A point is considered a peak if the detector output at this point is larger than that on the two adjacent beams. All peaks are replaced with a value of 1, while those outputs that are not peaks are set to zero. Therefore for this example, an ideal peak-picked plot would have ones at beams 20,30, and 80 and zeros elsewhere. The peak-picked responses are averaged over 1000 trials to obtain the figures. In this figure we note that the CAPE and SSMUSIC algorithms are both superior to the Capon algorithm and are roughly equivalent in terms of "detection" performance on the closely-spaced sources. This observation can be reconciled with the probability of resolution curves by observing that the SSMUSIC detector tends to place a peak on individual sources with the same frequency as does CAPE. However, SSMUSIC does not *simultaneously* place peaks on *both* sources as often as does CAPE.

The second experiment has the same parameters as

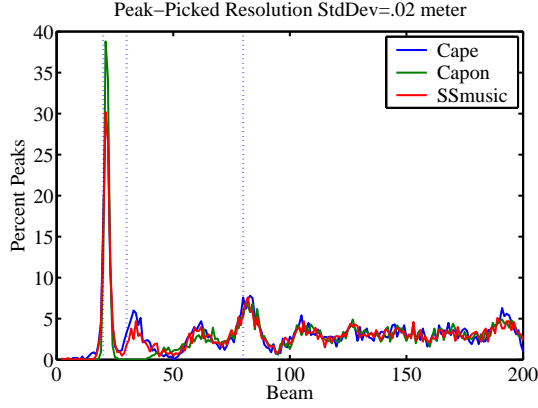


Figure 2: Peak-Picked Bearing Response

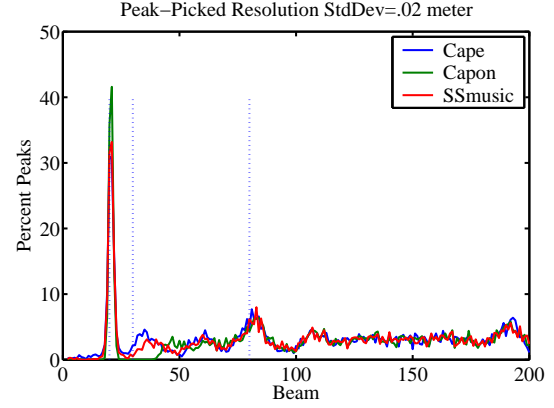


Figure 4: Peak-Picked Bearing Response: Beams 20 and 30 Correlated

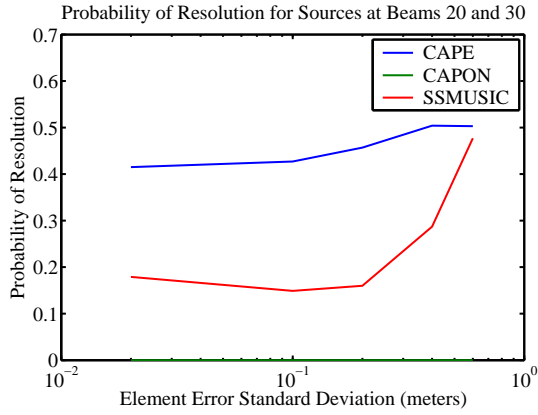


Figure 3: Probability of Resolution Results: Beams 20 and 30 Correlated

the first experiment except that the sources on beams 20 and 30 are correlated with a correlation coefficient  $\rho = 0.5e^{j\pi/7}$ . Again in this instance the CAPE detector has better resolution and detection performance in comparison to the CAPON algorithm and similar results to the SSMUSIC algorithm (which also has some multi-path mitigation [3]).

## 6. REFERENCES

- [1] L. L. Scharf and B. Friedlander, "Matched subspace detectors," *IEEE Trans. SP*, vol. 42, Aug. 1994.
- [2] R. O. Schmidt, *A signal subspace approach to multiple emitter location and spectral estimation*. PhD thesis, Stanford University, 1981.
- [3] M. L. McCloud and L. L. Scharf, "A new subspace identification algorithm for high-resolution DOA estimation," *IEEE Trans. Antennas Prop.*, vol. 50, Oct. 2002.

- [4] R. Schreiber, "Implementation of adaptive array algorithms," *IEEE Trans. ASSP*, vol. 34, pp. 1038–1045, Oct. 1986.
- [5] G. H. Golub and C. F. Van Loan, *Matrix Computations*. The Johns Hopkins University Press, 1989.



# Matched Detector “Philosophy”



- Filter data to remove everything but the signal-of-interest (SOI).
- Measure the “quantity” of what’s left.
  - If we started with an unknown quantity, take ratio of the filter output to initial quantity (CFAR).
- The filtering is not perfect – some interference can leak through.
  - Training data can be used to adjust the filter to minimize this leakage.
  - If training data contains the SOI, detector output suffers from suppression.
- **Matched Detector Summary**
  - Characterize the “background” (training data).
  - Do the test data “look like” SOI plus background or just background.
  - Suffer from background mismatch and signal suppression.



# A slightly-different approach



- Remove the SOI.
- Take the ratio of what's left over to what you started with.
- Interference can still cause misleading results
  - In this case if the interference is in the null of the matched filter.
- Use the testing data to provide information about the interference.
- **Summary**
  - Smaller interference mismatch than matched detectors
  - Accommodates SOI in data.
  - Is resistant to mismatch due to correlated signals (multi-path).



# Detector



- Through a series of monotonic transformations we arrive at the detector

$$d(a) = \frac{\sum_{i=r+1}^N \lambda_i(\hat{R})}{\sum_{i=r+1}^N \lambda_i((I - P_a)\hat{R}(I - P_a))}$$

- Here
  - $a$  is the SOL.
  - $\hat{R}$  is the sample covariance matrix (testing data).
  - $r$  is the rank of the dominant subspace of  $\hat{R}$ .
  - $\lambda_i(M)$  represents the  $i^{th}$  eigenvalue of  $M$ .

